Cell Reports
Physical Science

Article

Isomeric cues direct macrocycle selection from complex chemical systems for selective separation and recycling

Graphical abstract

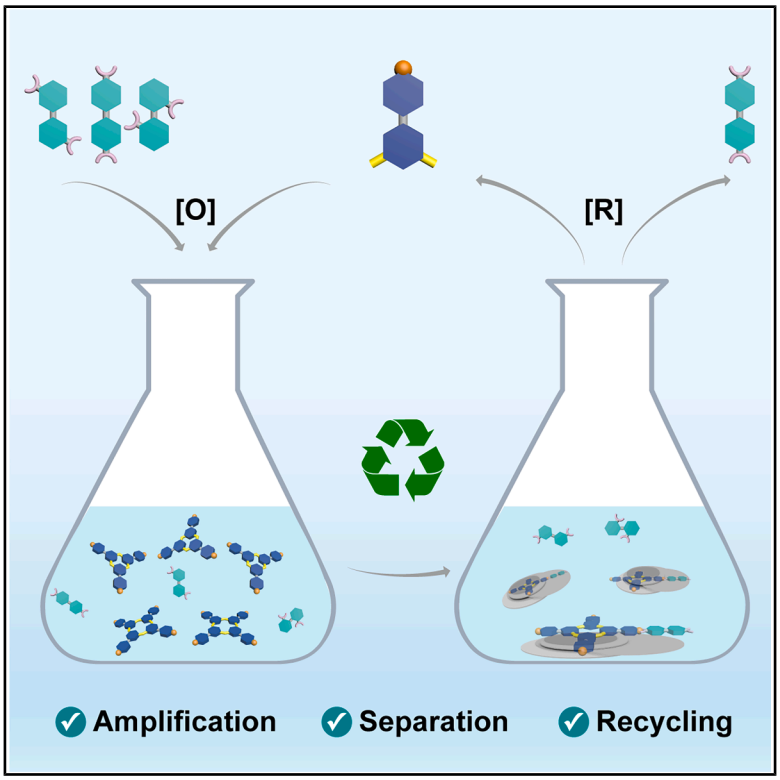

Authors

Xin Wang, Jinghui Yang, Emil Rosqvist, ..., Ermei Mäkilä, Fangyi Cheng, Jianwei Li

Correspondence

fycheng@nankai.edu.cn (F.C.), lijianwei@must.edu.mo (J.L.)

In brief

Wang et al. show that subtle isomeric differences can be amplified in a dynamic combinatorial system to direct selective macrocycle formation and self-assembly. Template-induced amplification generates ordered 2D nanosheets, enabling efficient separation and recyclability through precipitation.

Highlights

- Isomeric templates direct selective macrocycle amplification in a DCL
- Selective tetramer amplification drives ordered 2D nanosheet assembly
- Spontaneous precipitation enables efficient separation and recycling

Wang et al., 2026, Cell Reports Physical Science 7, 103140
March 18, 2026
https://doi.org/10.1016/j.xcrp.2026.103140

CellPress

Cell Reports
Physical Science

CellPress
OPEN ACCESS

Article

Isomeric cues direct macrocycle selection from complex chemical systems for selective separation and recycling

Xin Wang,[1,2,3] Jinghui Yang,[1,2,3] Emil Rosqvist,[4] Yonglei Lyu,[1,2,3] Anastassios C. Papageorgiou,[5] Jouko Peltonen,[4] Ermei Mäkilä,[6] Fangyi Cheng,[7,*] and Jianwei Li[1,8,*]

[1]Macao Institute of Materials Science and Engineering (MIMSE), Faculty of Innovation Engineering, Macau University of Science and Technology, Taipa, Macao 999078, China
[2]Department of Chemistry, University of Turku, 20500 Turku, Finland
[3]MediCity Research Laboratory, University of Turku, 20520 Turku, Finland
[4]Physical Chemistry, Laboratory of Molecular Science and Engineering, Åbo Akademi University, 20520 Turku, Finland
[5]Turku Bioscience Centre, University of Turku, Åbo Akademi University, 20520 Turku, Finland
[6]Laboratory of Industrial Physics, Department of Physics and Astronomy, Institute of Dentistry, University of Turku, 20014 Turku, Finland
[7]College of Chemistry, Nankai University, Tianjin, China
[8]Lead contact
*Correspondence: fycheng@nankai.edu.cn (F.C.), lijianwei@must.edu.mo (J.L.)
https://doi.org/10.1016/j.xcrp.2026.103140

SUMMARY

Living systems translate subtle molecular variations into functional complexity through selective recognition and hierarchical self-assembly. Here, we report that dynamic combinatorial chemistry (DCC) can amplify minute structural differences among isomeric templates, guiding templated selection toward distinct supramolecular outcomes. Using a dithiol building block, a library of macrocycles is generated, within which only one isomeric template selectively amplifies the tetrameric macrocycle. Their co-assembly produces highly ordered 2D nanosheets that spontaneously precipitate, enabling facile component separation. This selective organization contrasts with the simple 1:1 complex formed by other isomers, underscoring the sensitivity of dynamic systems to small structural cues. Significantly, both the template and the amplified species are recovered with high efficiency, allowing material recyclability. These findings reveal how dynamic molecular systems transform subtle information into functional architectures, offering a conceptual model for templated selection and a strategy for the design of adaptive supramolecular materials featuring selective recognition, separation, and reuse.

INTRODUCTION

Living systems are renowned for their unparalleled complexity and sophistication,[1] at the core of which lie precise molecular recognition,[2–4] programmed bottom-up self-assembly,[5,6] and the capacity for selective adaptation through natural processes.[7–10] These processes operate synergistically, enabling organisms to construct highly ordered structures and dynamic networks with specific functions from relatively simple chemical building blocks.[11–13] Understanding the fundamental chemical principles by which information is encoded, transmitted, amplified, and ultimately translated into functional architecture within these complex life processes remains one of the central challenges in contemporary science, crucial for simulating and reconstructing life's characteristics at the molecular level.[14–16]

To explore these fundamental principles, chemists strive to construct artificial chemical systems capable of mimicking key features of biological systems.[17,18] Dynamic Combinatorial Chemistry (DCC) has emerged as a powerful research tool in this endeavor.[19,20] In dynamic combinatorial libraries (DCLs), component molecules continuously form and break reversible chemical bonds, with the entire system operating under thermodynamic control.[21–23] This allows library members to self-adjust, select, and undergo templated selection or adaptive reorganization in response to internal or external stimuli (such as the presence of a template), thereby enriching the components best adapted to the current environment.[24–26] This mechanism of dynamic selection and amplification bears a profound resemblance to the "survival of the fittest" principle in biological systems, offering an ideal platform for simulating templated selection and adaptive behaviors under laboratory conditions.[27,28]

In true biological adaptation and self-organization, subtle structural differences between molecules can often lead to vast divergence in their biological functions and fates.[29] For instance, a minor change at a single chiral center or functional group in a protein or nucleic acid can significantly impact its recognition, binding, catalytic, or assembly properties, leading to its selection or elimination in a competitive environment.[30–32]

Please cite this article in press as: Wang et al., Isomeric cues direct macrocycle selection from complex chemical systems for selective separation and recycling, Cell Reports Physical Science (2026), https://doi.org/10.1016/j.xcrp.2026.103140

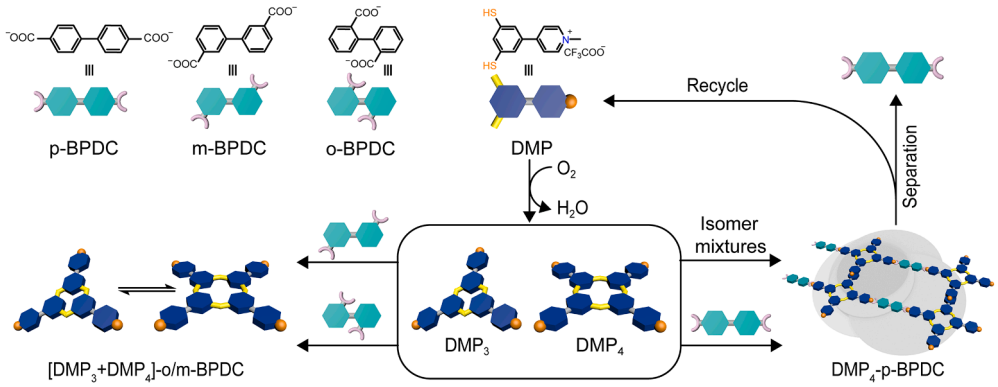

Scheme 1. Dynamic combinatorial selection and isomer separation

A DCL (DMP_3 and DMP_4) from DMP oxidation by air: selective recognition of *p*-BPDC among three isomeric carboxylic acids and subsequent separation from the mixture.

However, in artificial chemical systems, how to precisely harness and amplify such minute structural information, driving the selective amplification of specific chemical species through competitive templating effects, and further guiding their self-assembly into higher-order, functional structures emulating the adaptive hierarchical organization observed in biological systems remains a subject requiring intensive investigation.[25,33,34]

Separation is a central process in chemistry and materials science, enabling purification, recovery, and reuse of valuable components.[35] Conventional separation technologies, including chromatography,[36] adsorption on porous materials such as metal-organic frameworks (MOFs)[37] and covalent organic frameworks (COFs),[38] membrane filtration,[39] and liquid-liquid extraction,[40] have achieved remarkable efficiency but generally rely on external gradients, fixed interfaces, or solvent- and energy-intensive operations. Chromatography remains the most versatile and widely used technique for molecular purification, but its dependence on continuous flow and stationary phases limits intrinsic adaptability and recyclability. These methods excel in large-scale or routine separations but are less suited for systems requiring dynamic molecular recognition or reversible reorganization. In contrast, DCC offers an intrinsically adaptive, thermodynamically controlled route to molecular differentiation. Within a DCC network, reversible covalent exchange allows both the template and the library components to influence each other, leading to mutual selection and amplification of the most compatible species.[17,41] Such reciprocal recognition enables selective co-assembly and spontaneous phase separation, converting subtle structural differences into macroscopic isolation and component recovery under mild, aqueous, and environmentally benign conditions, providing a green and recyclable approach for adaptive molecular separation.

In the present study (Scheme 1), we introduce a mixture of structurally highly similar isomers as templates into a DCL, aiming to investigate how subtle molecular structural differences can influence the templated selection pathways and self-assembly behaviors of chemical species in a competitive environment. We discovered that a specific chemical component within the system underwent significant quantitative amplification due to its specific co-assembly with one particular isomer from the template mixture, leading to the formation of a well-ordered supramolecular 2D copolymer film. Significantly, these resultant films can be conveniently separated as precipitates from the aqueous phase using centrifugation. Taking advantage of the supramolecular nature of this material, the particular templating isomer can be subsequently extracted with 96% purity, and the amplified library species can also be isolated for recovery to the original building block. The building block could be reused in subsequent separation cycles without loss of performance. In stark contrast, other structurally very similar isomeric templates, despite also being able to interact with this chemical component or other library members, only formed a simple 1:1 supramolecular complex and failed to induce similar amplification or the formation of distinct supramolecular assemblies exhibiting selective precipitation behavior.

This study demonstrates how dynamic complex systems amplify subtle molecular differences (e.g., between isomers) through competitive templating and selective self-assembly. This process drives adaptive amplification and organization into higher-order supramolecular structures with specific functions, as shown here, and practical benefits like component separability and recyclability. Such spontaneous organization from a mixture to a functional entity exemplifies how molecular information can be translated into ordered structures via selective recognition and assembly. We elucidate the underlying mechanisms, discussing their implications for simulating biological self-organization and adaptive processes and for advancing the on-demand design of functional supramolecular materials featuring efficient component recovery and application.

RESULTS

Synthesis of the building block and oxidized library

We first designed and synthesized a dithiol building block, 4-(3,5-dimercaptophenyl)-1-methylpyridin-1-ium (DMP) (Figures 1 and S1–S20) and used it (2.4 mM) to prepare a library in PBS buffer (50 mM [pH 7.4]). The library was stirred in air for 7 days to ensure complete oxidation. High-performance liquid chromatography-mass spectrometry (HPLC-MS) analysis (Figures 2A, S21, and S22) revealed two distinct peaks corresponding to trimeric (DMP_3) and tetrameric (DMP_4) macrocycles. Their synthesis

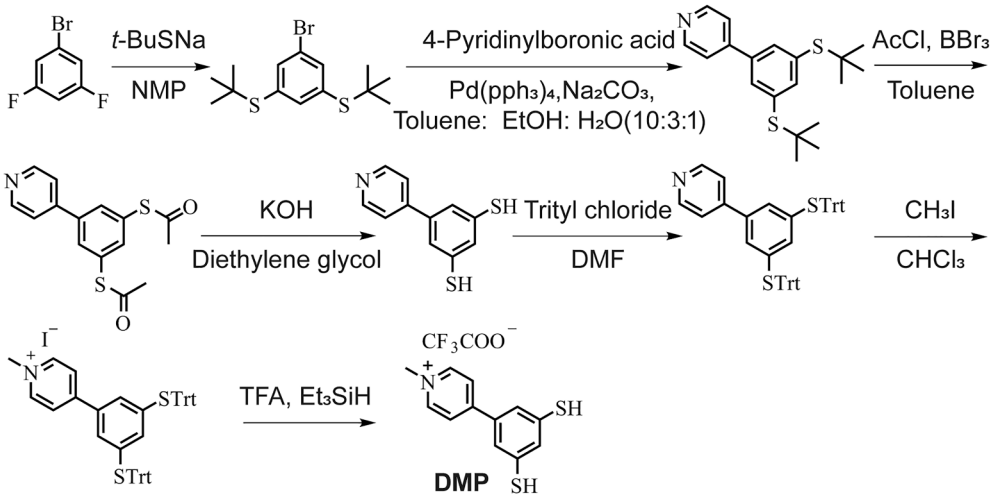

Figure 1. Synthetic route of the building block DMP

Shown is a schematic of the synthesis pathway leading to the preparation of DMP.

was also characterized using proton nuclear magnetic resonance (^{1}H-NMR) spectroscopy (Figure S23).

Selective recognition of *p*-BPDC by the DCL

To investigate the recognition selectivity of the DCL toward structurally related isomeric templates, namely biphenyl-4,4′-dicarboxylic acid, biphenyl-3,3′-dicarboxylic acid, and biphenyl-2,2′-dicarboxylic acid (*p*-, *m*-, and *o*-BPDC, respectively), three parallel libraries were constructed by combining DMP (2.4 mM) with either *p*-, *m*-, or *o*-BPDC (1.2 mM each). Upon complete oxidation, only the *p*-BPDC-containing library became cloudy (Figure S24). Although this change in transparency provided visual confirmation

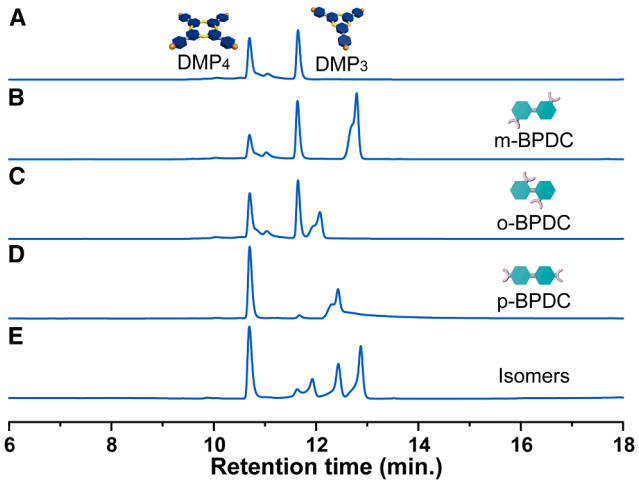

Figure 2. HPLC-MS analysis of dynamic libraries with or without isomeric templates

Shown are the fully oxidized libraries made (A) from the building block DMP (2.4 mM) without any template and with template (B) *m*-BPDC (1.2 mM), (C) *o*-BPDC (1.2 mM), (D) *p*-BPDC (1.2 mM), and (E) isomer mixtures containing *o*-BPDC (1.2 mM), *p*-BPDC (1.2 mM), and *m*-BPDC (1.2 mM) in 50 mM PBS buffer (pH 7.4).

of selective recognition, we conducted further analysis. HPLC-MS analysis revealed that *p*-BPDC selectively promoted the amplification of the tetramer DMP_4, whereas libraries with *m*-BPDC or *o*-BPDC showed no significant component changes compared to the control library (Figures 2A–2D and S25). To confirm that the species amplified by *p*-BPDC was indeed DMP_4, the library was purified by preparative HPLC, and the subsequent ^{1}H-NMR spectrum matched the previous data (Figures 3A and S26). The selectivity under competitive conditions was evaluated by preparing a library from an equimolar mixture of *p*-, *m*-, and *o*-BPDC (1.2 mM each) with the building block DMP. Upon complete oxidation, the solution became turbid, and HPLC-MS analysis revealed that the tetramer was still markedly amplified (Figure 2E). These findings demonstrate that, even in the presence of structurally similar competitors, *p*-BPDC is selectively incorporated into the supramolecular assembly, highlighting the capability of DCL to amplify subtle structural differences via competitive templating. Further analysis revealed additional features that influence the amplification behavior. In this system, only *p*-BPDC directs the library toward enrichment of the tetramer, and the amplification outcome is also affected by the aggregation behavior of the resulting complexes. Concentration-dependent DCL experiments showed that the extent of DMP_4 amplification increases with the total concentration in a cooperative manner (Figure S27), and this cooperative behavior likely arises because template binding and aggregation act in a mutually reinforcing manner. Self-dilution studies of the pre-formed DMP_4-*p*-BPDC complex confirmed that aggregation occurs at low micromolar concentrations (Figure S28). These observations indicate that both template-macrocycle binding and aggregation contribute to the final composition of the DCL.

Binding interactions between BPDC isomers and macrocycles

The interaction between DMP_4 and DMP_3 with BPDC isomers was characterized by ^{1}H-NMR (Figure 3B). The peaks of H1-4 on *o*-BPDC or *m*-BPDC shifted upfield, while *p*-BPDC showed

CellPress
OPEN ACCESS

Cell Reports
Physical Science
Article

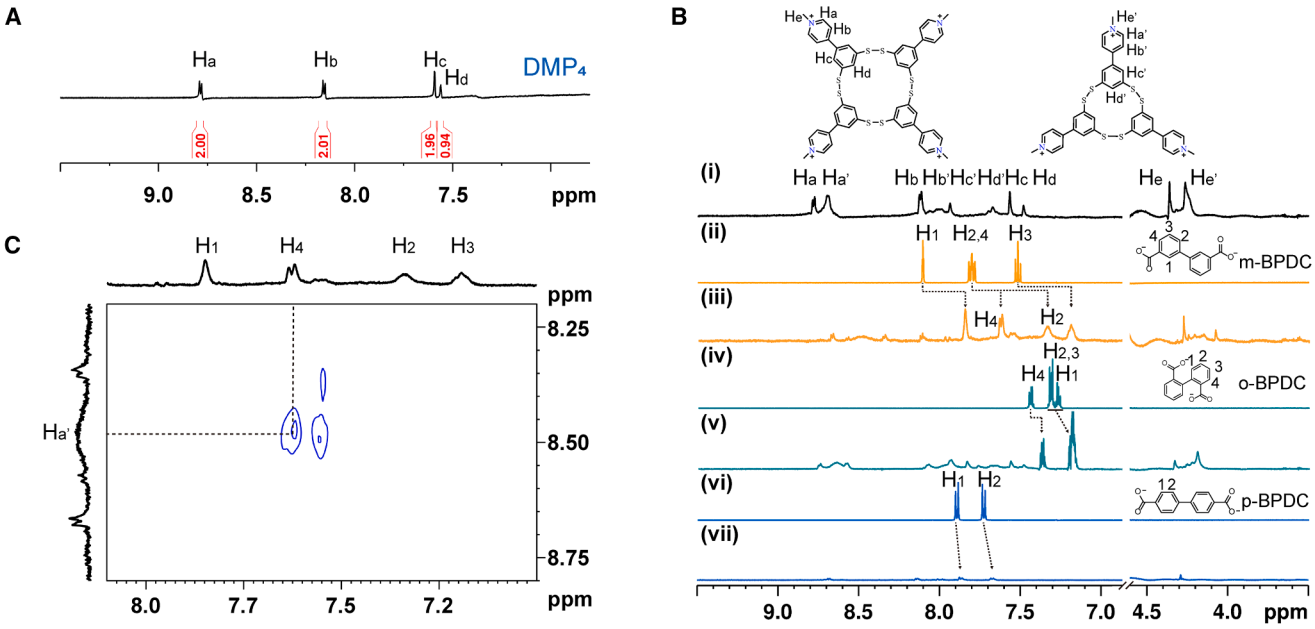

Figure 3. NMR spectra of dynamic libraries and recognition with BPDC isomers

(A) Partial ^{1}H-NMR spectrum of DMP_4 purified by semi-preparative column separation. (D_2O/H_2O = 2/3, 600 MHz, 298 K).

(B) ^{1}H-NMR spectra (500 MHz, D_2O/H_2O = 3/2, 20 mM PBS buffer [pH 7.4], 298 K): (i) the fully oxidized libraries made from building block DMP (2.0 mM); (ii) 1.0 mM *m*-BPDC; (iii) the fully oxidized libraries made from building block DMP 2.0 mM and 1.0 mM *m*-BPDC; (iv) 1.0 mM *o*-BPDC; (v) the fully oxidized libraries made from building block DMP 2.0 mM and 1.0 mM *o*-BPDC; (vi) 1.0 mM *p*-BPDC; and (vii) the fully oxidized libraries made from building block DMP 2.0 mM and 1.0 mM *p*-BPDC.

(C) Partial 2D NOESY spectrum of the fully oxidized libraries made from building block DMP 2.0 mM and 1.0 mM *m*-BPDC.

a slight upfield shift of H1-2 accompanied by a reduction in signal intensity. In particular, the Ha′ on DMP_3 exhibited splitting and chemical shift changes upon interaction with *o*-BPDC, whereas the corresponding changes in DMP_4 were less changed. Furthermore, the two-dimensional nuclear Overhauser effect spectroscopy (2D NOESY) spectrum showed the correlation signal between protons H4 on *m*-BPDC and Ha′ on DMP_3, H2-3 on *o*-BPDC, and Hd′ on DMP_3 (Figures 3C, S29A, and S29B). Diffusion-ordered spectroscopy (DOSY) NMR (Figure S29D) showed that DMP_3 and DMP_4 co-diffused with *o*-BPDC, with diffusion coefficients slightly reduced relative to the free species (Figures S23C and S29F), indicating complex formation without large aggregation.[42] The interaction between *p*-BPDC and DMP_4 resulted in precipitation, and the NMR signals were too weak to allow acquisition of reliable NOESY or DOSY spectra. We then used DCLfit to evaluate how the different BPDC isomers influence the DCL composition (Tables S1, S2, S3, and S4; Figures S30–S33).[43] Because the DMP_4-*p*-BPDC system undergoes aggregation within the DCL, the fitted values cannot be interpreted as intrinsic binding constants.[44] Instead, they reflect the overall equilibrium bias exerted by each template. As shown in Table S5, *p*-BPDC imposes a much stronger bias toward DMP_4 than toward DMP_3, consistent with the absence of DMP_3 in its presence. By contrast, *o*-BPDC and *m*-BPDC exert only weak influence on the tetramer. Although NMR analyses revealed interactions of *o*- and *m*-BPDC with the trimer, these interactions did not translate into a clear templating effect. These results indicate that only *p*-BPDC provides sufficient molecular recognition and aggregation under the DCL conditions to drive selective tetramer amplification, whereas the minimal impact of *o*-BPDC and *m*-BPDC does not result in a templating effect.

Structural characterization of nanosheets formed by *p*-BPDC and DMP_4

Since the strong binding between *p*-BPDC and DMP_4 led to precipitation in the library, we investigated the morphology of the aggregates using transmission electron microscopy (TEM) and scanning electron microscopy (SEM), revealing the formation of 2D nanosheets with an approximate diameter of 1,000 nm (Figures 4A; Figure S34A), in good agreement with the relative size distribution obtained from dynamic light scattering (DLS) measurements (Figure S34B). Atomic force microscopy (AFM) analysis showed a 7-layer thickness ranging from 0.5 to 14 nm (Figure 4B) with an average monolayer thickness of ~1.9 nm, indicating that these nanosheets possess ultrathin characteristics. The uniform thickness suggests an ordered molecular arrangement. Powder X-ray diffraction (PXRD) analysis further supported these findings (Figure 4C), showing peaks at 5.05° and 22.6°, corresponding to d spacings of 17.5 and 3.9 Å, which align with the thickness measured by AFM and the π-π stacking interactions,[45] respectively. The Pawley refinement was conducted on the experimental diffraction pattern, revealing unit cell parameters of a = 64.773 Å, b = 48.639 Å, c = 7.600 Å, α = 90.16°, β = 90.59°, and γ = 88.26°, with profile R-factor (Rp) = 0.73% and weighted profile R-factor (Rwp) = 3.48%

Please cite this article in press as: Wang et al., Isomeric cues direct macrocycle selection from complex chemical systems for selective separation and recycling, Cell Reports Physical Science (2026), https://doi.org/10.1016/j.xcrp.2026.103140

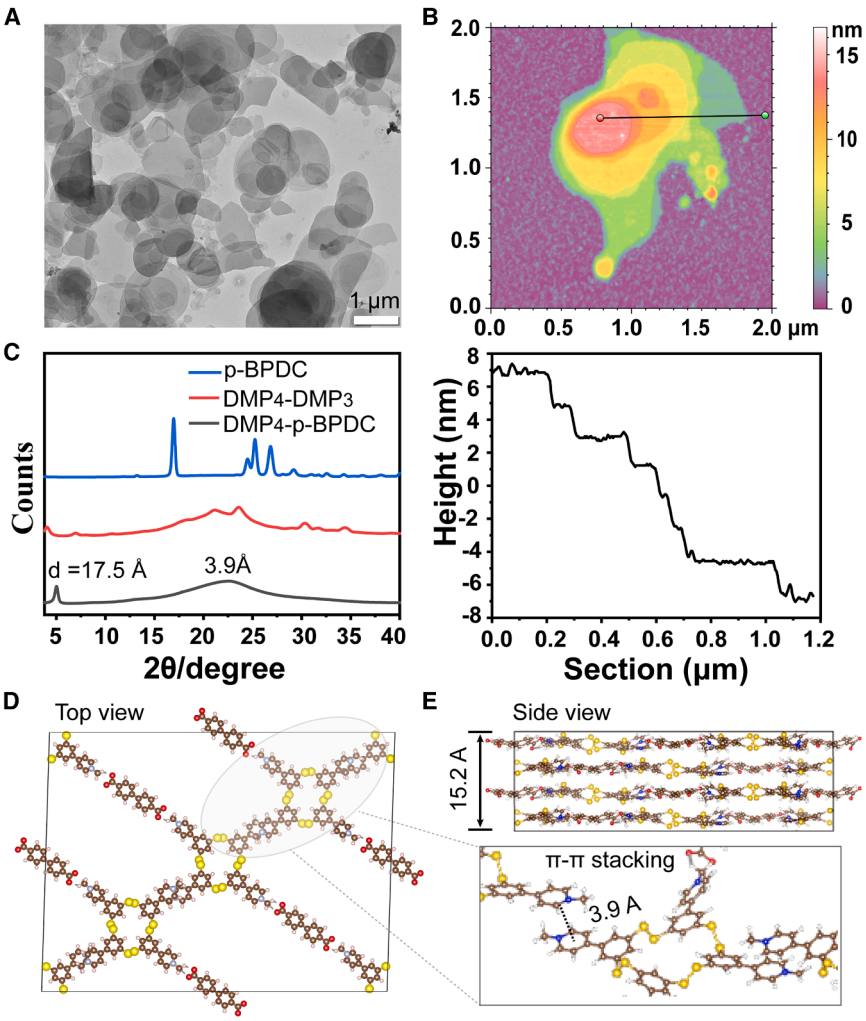

Figure 4. Characterization of DMP4-*p*-BPDC 2D nanosheets

(A) TEM image of DMP_4-*p*-BPDC (scale bar: 1 μm).

(B) Atomic force microscopy (AFM) image and corresponding height profile of DMP_4-*p*-BPDC. Scan size is 2 × 2 μm.

(C) PXRD patterns of the DMP_4-*p*-BPDC 2D nanosheets (black line), DMP_4-DMP_3 (red line), and *p*-BPDC (blue line).

(D) Simulated stacking model for 2D nanosheet in top view (view along the *c* axis; color ball scheme: C, gray; O, red; N, blue; H, light pink; S, yellow). See also Table S6.

(E) Front view (view along the *a* axis) of a 2D nanosheet, displaying two-unit cells. The bottom presents a magnified view of a localized region of d, highlighting the structural details.

(Figure S35; Table S6). These observations align with the simulated structure (Figure 4D), which exhibits an AB stacking arrangement. The refined lattice constant c = 0.76 nm suggests a multilayer stacking along the *c* axis. Using N = d/c, the estimated N ≈ 2.3 suggests a predominant bilayer stacking arrangement.[46] The calculated 2c value of 15.2 Å (Figure 4E) closely matches the experimentally observed d spacing by XRD. The combination of XRD, AFM, and electron microscopy confirms that these nanosheets adopt a well-ordered layered architecture (arrangement model shown in Figure 4E).

Separation and recycling in the *p*-BPDC-DMP_4 system

Encouraged by the selective precipitation between the DCL and the acid isomer mixture, as confirmed by HPLC after centrifugation showing DMP_4 and *p*-BPDC as the major components in the precipitate and the unreacted acids in the supernatant (Figure S36), we explored isolating *p*-BPDC from the supramolecular co-assemblies. Since electrostatic interactions are key to binding, we hypothesized that lowering the pH would protonate the carboxyl groups of *p*-BPDC, disrupting its interaction with DMP_4. This would render *p*-BPDC insoluble while leaving DMP_4 unaffected, allowing for purification via filtration. However, this approach was unsuccessful (Figure S37A), likely due to the strong multivalent interaction between *p*-BPDC and DMP_4. We then sought to disrupt the tetramer into its monomeric form to weaken the binding affinity. Adding DTT (in an amount equivalent to the disulfide bonds) to the mixture successfully reduced the disulfide bonds. After 2 h, the pH was adjusted to 2 using trifluoroacetic acid, causing *p*-BPDC to precipitate. The precipitation was isolated via centrifugation, and HPLC analysis confirmed 96% purity of *p*-BPDC (Figure S37B; Table S7) in the first separation process. In addition, the supernatant contained the reduced DMP_4, which reverted to the building block, ready for reuse in extracting *p*-BPDC, and this recycling process could be repeated at least three times without loss of performance (Figures 5A and S38). The average purity of *p*-BPDC was 96% in three extraction cycles (Table S7). The recycling rate of the building block was over 93%, demonstrating the recyclability of the system. The isolation process of *p*-BPDC from its isomer mixture is shown in Figure 5B.

DISCUSSION

This work demonstrates that subtle structural differences among isomeric templates can be amplified within a DCL, directing the system toward distinct self-assembly outcomes. Through competitive templating, *p*-BPDC selectively amplified the tetrameric macrocycle DMP_4. When assembled individually with *p*-BPDC, DMP_4 formed highly ordered 2D nanosheets that could serve as a supramolecular platform for the efficient separation of *p*-BPDC. In contrast, other closely related isomers formed only simple 1:1 complexes and failed to induce comparable amplification or ordered architectures. These findings highlight the ability of dynamic complex systems to transform minute

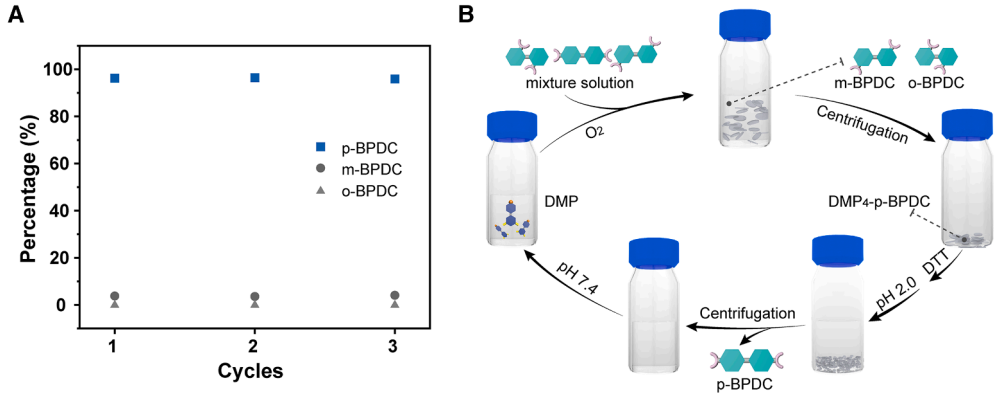

Figure 5. Selective separation of BPDC isomers by DCC

(A) Percentage of *p*-BPDC, *m*-BPDC, and *o*-BPDC separated by DCC during three recycling cycles.

(B) Schematic of the selective separation process of *p*-BPDC, *m*-BPDC, and *o*-BPDC by the DCC.

molecular distinctions into pronounced structural and functional divergences, providing insights into the chemical principles of templated selection and the design of adaptive supramolecular materials with integrated separation capabilities. While this study primarily focuses on model isomeric systems, the general applicability of this strategy remains to be explored. Future efforts will aim to extend this dynamic separation approach toward the selective capture and treatment of fluorescent dyes and related organic pollutants as well as the recognition and purification of negatively charged functional biomolecules.

METHODS

Materials

All reagents and solvents used for synthesis and analysis were commercially available without further purification unless otherwise noted. Key organic compounds (*p*-BPDC, *m*-BPDC, and *o*-BPDC) and other reagents were obtained from Sigma-Aldrich or TCI. Solvents were of analytical or HPLC grade.

General synthesis and purification procedures

Chemical synthesis and sample preparation were carried out using standard laboratory techniques. Purification was performed using a BUCHI automated flash chromatography system equipped with pre-packed columns with Agela flash column silica-CS.

Characterization

^{1}H-, ^{13}C-NMR spectra, as well as correlation spectroscopy (COSY), NOESY, DOSY, heteronuclear single-quantum coherence (HSQC), and heteronuclear multiple-bond correlation (HMBC) experiments, were recorded on Bruker AV500, AV500 cryo, and AV600 cryo spectrometers at 298 K. HSQC experiments were conducted using the hsqcetgp pulse program. HMBC experiments were conducted using the hmbcetgpl3nd pulse program. Mass spectroscopy was performed on Waters RDa Accurate Mass. The morphology of the nanosheets was characterized by TEM (JEM-1400 Plus, JEOL, Japan) and field emission SEM (FE-SEM; Thermo Scientific Apreo S). The sample size measurements were performed using a Zeta Nano-ZS instrument by Malvern equipped with a 633 nm He-Ne laser. AFM imaging was performed using a Nanoscope Multimode 8 (Bruker, MA, USA) using PeakForce mode. Measurements were conducted at temperature (T) = 23 ± 2°C and relative humidity (RH) = 30% ± 2% using ScanAsystAir cantilevers (Bruker). These cantilevers had spring constants in the range of 0.27–0.43 N/m and a nominal tip radius of 2 nm. Image processing (line-by-line, least-squares plane, or three-point plane flattening) and analysis were done with MountainsSPIP (version 9.3.10663; DigitalSurf, Besançon, France). XRD experiments were conducted using a MicroMax 007 HF X-ray generator equipped with a HyPix-6000HE photon counting detector. UV-visible (UV-vis) absorption spectra were recorded on a Shimadzu UV-1900i UV-vis spectrophotometer. HPLC analyses were performed on an Ultimate 3000 system equipped with a photodiode array (PDA) detector.

Selective separation and recycling experiments

Selective separation of *p*-BPDC from a mixture of positional isomers was carried out using a template-mediated redox process in aqueous buffer. Oxidation-induced complex formation resulted in selective precipitation, followed by reductive release of *p*-BPDC and pH-controlled recovery of the free acid. The separation process was repeated in multiple cycles to evaluate recyclability. The composition of the precipitated and released fractions was analyzed by HPLC. Further details regarding the methods can be found in the supplemental information.

RESOURCE AVAILABILITY

Lead contact

Requests for further information and resources should be directed to and will be fulfilled by the lead contact, Jianwei Li (lijianwei@must.edu.mo).

Materials availability

This study did not generate new unique reagents.

Data and code availability

- The data supporting this study are available in the manuscript and supplemental information.

- This paper does not report original code.
- Any additional information required to reanalyze the data reported in this paper is available from the lead contact upon request.

ACKNOWLEDGMENTS

We are grateful for financial support from the National Natural Science Foundation of China (22161016) and Sigrid Jusélius Foundation (Senior Researcher Fellowship). X.W. and J.Y. acknowledge support from the China Scholarship Council. We thank the Turku Center for Chemical and Molecular Analytics for providing NMR and MS and the Electron Microscopy Laboratory, Institute of Biomedicine, University of Turku, and Biocenter Finland for TEM imaging. We also thank Prof. Sijbren Otto (University of Groningen) for generously providing the DCLfit software, which was used for determining the affinity constants between macrocycles and isomeric templates in the library.

AUTHOR CONTRIBUTIONS

X.W. designed the project, performed the experiments, and wrote the manuscript. J.Y. assisted with the synthesis and supported data analysis. E.R. and J.P. performed the AFM measurements and analysis. Y.L. contributed to MS analysis. A.C.P. conducted the PXRD characterization. E.M. performed the SEM measurement. F.C. supervised the concentration effects on oxidative amplification and revised the manuscript. J.L. conceived the idea, supervised the research, and revised the manuscript.

DECLARATION OF INTERESTS

The authors declare no competing interests.

SUPPLEMENTAL INFORMATION

Supplemental information can be found online at https://doi.org/10.1016/j.xcrp.2026.103140.

Received: October 6, 2025
Revised: December 2, 2025
Accepted: January 20, 2026

REFERENCES

1. Wolf, Y.I., Katsnelson, M.I., and Koonin, E.V. (2018). Physical foundations of biological complexity. Proc. Natl. Acad. Sci. USA *115*, E8678–E8687. https://doi.org/10.1073/pnas.1807890115.
2. de Jong, J., Bos, J.E., and Wezenberg, S.J. (2023). Stimulus-controlled anion binding and transport by synthetic receptors. Chem. Rev. *123*, 8530–8574. https://doi.org/10.1021/acs.chemrev.3c00039.
3. Escobar, L., and Ballester, P. (2021). Molecular Recognition in Water Using Macrocyclic Synthetic Receptors. Chem. Rev. *121*, 2445–2514. https://doi.org/10.1021/acs.chemrev.0c00522.
4. Fu, R., Zhao, Q.Y., Han, H., Li, W.L., Chen, F.Y., Tang, C., Zhang, W., Guo, S.D., Li, D.Y., Geng, W.C., et al. (2023). A Chiral Emissive Conjugated Corral for High-Affinity and Highly Enantioselective Recognition in Water. Angew. Chem. Int. Ed. *62*, e202315990. https://doi.org/10.1002/anie.202315990.
5. De Greef, T.F.A., Smulders, M.M.J., Wolffs, M., Schenning, A.P.H.J., Sijbesma, R.P., and Meijer, E.W. (2009). Supramolecular Polymerization. Chem. Rev. *109*, 5687–5754. https://doi.org/10.1021/cr900181u.
6. Zhan, P., Peil, A., Jiang, Q., Wang, D., Mousavi, S., Xiong, Q., Shen, Q., Shang, Y., Ding, B., Lin, C., et al. (2023). Recent Advances in DNA Origami-Engineered Nanomaterials and Applications. Chem. Rev. *123*, 3976–4050. https://doi.org/10.1021/acs.chemrev.3c00028.
7. Weißenfels, M., Gemen, J., and Klajn, R. (2021). Dissipative Self-Assembly: Fueling with Chemicals versus Light. Chem *7*, 23–37. https://doi.org/10.1016/j.chempr.2020.11.025.
8. Das, K., Gabrielli, L., and Prins, L.J. (2021). Chemically fueled self-assembly in biology and chemistry. Angew. Chem. Int. Ed. *60*, 20120–20143. https://doi.org/10.1002/anie.202100274.
9. Sorrenti, A., Leira-Iglesias, J., Markvoort, A.J., de Greef, T.F.A., and Hermans, T.M. (2017). Non-equilibrium supramolecular polymerization. Chem. Soc. Rev. *46*, 5476–5490. https://doi.org/10.1039/c7cs00121e.
10. Ashkenasy, G., Hermans, T.M., Otto, S., and Taylor, A.F. (2017). Systems chemistry. Chem. Soc. Rev. *46*, 2543–2554. https://doi.org/10.1039/c7cs00117g.
11. Ruiz-Mirazo, K., Briones, C., and de la Escosura, A. (2014). Prebiotic systems chemistry: new perspectives for the origins of life. Chem. Rev. *114*, 285–366. https://doi.org/10.1021/cr2004844.
12. Singh, A., Parvin, P., Saha, B., and Das, D. (2024). Non-equilibrium self-assembly for living matter-like properties. Nat. Rev. Chem *8*, 723–740. https://doi.org/10.1038/s41570-024-00640-z.
13. Frenkel-Pinter, M., Samanta, M., Ashkenasy, G., and Leman, L.J. (2020). Prebiotic peptides: Molecular hubs in the origin of life. Chem. Rev. *120*, 4707–4765. https://doi.org/10.1021/acs.chemrev.9b00664.
14. Walter, V., Bi, D., Salehi-Reyhani, A., and Deng, Y. (2023). Real-time signal processing via chemical reactions for a microfluidic molecular communication system. Nat. Commun. *14*, 7188. https://doi.org/10.1038/s41467-023-42885-0.
15. Ding, L., Chen, X., Ma, W., Li, J., Liu, X., Fan, C., and Yao, G. (2023). DNA-mediated regioselective encoding of colloids for programmable self-assembly. Chem. Soc. Rev. *52*, 5684–5705. https://doi.org/10.1039/d2cs00845a.
16. Robinson, W.E., Daines, E., van Duppen, P., de Jong, T., and Huck, W.T.S. (2022). Environmental conditions drive self-organization of reaction pathways in a prebiotic reaction network. Nat. Chem. *14*, 623–631. https://doi.org/10.1038/s41557-022-00956-7.
17. Lehn, J.M. (2007). From supramolecular chemistry towards constitutional dynamic chemistry and adaptive chemistry. Chem. Soc. Rev. *36*, 151–160. https://doi.org/10.1039/b616752g.
18. Aguanell, A., Hennebelle, M., Ortega, M.Á., and Pérez-Fernández, R. (2025). Dynamic combinatorial chemistry directed by proteins and nucleic acids: a powerful tool for drug discovery. Chem. Soc. Rev. *54*, 7093–7113. https://doi.org/10.1039/d5cs00223k.
19. Corbett, P.T., Leclaire, J., Vial, L., West, K.R., Wietor, J.L., Sanders, J.K.M., and Otto, S. (2006). Dynamic combinatorial chemistry. Chem. Rev. *106*, 3652–3711. https://doi.org/10.1021/cr020452p.
20. Cougnon, F.B.L., and Sanders, J.K.M. (2012). Evolution of Dynamic Combinatorial Chemistry. Acc. Chem. Res. *45*, 2211–2221. https://doi.org/10.1021/ar200240m.
21. Belowich, M.E., and Stoddart, J.F. (2012). Dynamic imine chemistry. Chem. Soc. Rev. *41*, 2003–2024. https://doi.org/10.1039/c2cs15305j.
22. Pérez-Fernández, R., Pittelkow, M., Belenguer, A.M., Lane, L.A., Robinson, C.V., and Sanders, J.K.M. (2009). Two-phase dynamic combinatorial discovery of a spermine transporter. Chem. Commun., 3708–3710. https://doi.org/10.1039/b902842k.
23. Yang, J., Wang, X., Wu, X., Lyu, Y., Papageorgiou, A.C., and Li, J. (2025). Quantitative synthesis of dynamic combinatorial macrocycles accelerated by preorganization of AIEgens for live visualization of drug release. Cell Rep. Phys. Sci. *6*, 102355. https://doi.org/10.1016/j.xcrp.2024.102355.
24. Li, J., Nowak, P., and Otto, S. (2013). Dynamic Combinatorial Libraries: From Exploring Molecular Recognition to Systems Chemistry. J. Am. Chem. Soc. *135*, 9222–9239. https://doi.org/10.1021/ja402586c.
25. Kriebisch, C.M.E., Burger, L., Zozulia, O., Stasi, M., Floroni, A., Braun, D., Gerland, U., and Boekhoven, J. (2024). Template-based copying in chemically fuelled dynamic combinatorial libraries. Nat. Chem. *16*, 1240–1249. https://doi.org/10.1038/s41557-024-01570-5.

26. Casciuc, I., Osypenko, A., Kozibroda, B., Horvath, D., Marcou, G., Bonachera, F., Varnek, A., and Lehn, J.M. (2022). Toward in Silico Modeling of Dynamic Combinatorial Libraries. ACS Cent. Sci. *8*, 804–813. https://doi.org/10.1021/acscentsci.2c00048.

27. Diehl, C.J., Salerno, A., and Ciulli, A. (2024). Ternary Complex-Templated Dynamic Combinatorial Chemistry for the Selection and Identification of Homo-PROTACs. Angew. Chem. Int. Ed. *63*, e202319456. https://doi.org/10.1002/anie.202319456.

28. Otto, S. (2022). An Approach to the De Novo Synthesis of Life. Acc. Chem. Res. *55*, 145–155. https://doi.org/10.1021/acs.accounts.1c00534.

29. Hastings, R., Aditham, A.K., DelRosso, N., Suzuki, P.H., and Fordyce, P.M. (2025). Mutations to transcription factor MAX allosterically increase DNA selectivity by altering folding and binding pathways. Nat. Commun. *16*, 636. https://doi.org/10.1038/s41467-024-55672-2.

30. Aubrey, L.D., Ninkina, N., Ulamec, S.M., Abramycheva, N.Y., Vasili, E., Devine, O.M., Wilkinson, M., Mackinnon, E., Limorenko, G., Walko, M., et al. (2024). Substitution of Met-38 to Ile in γ-synuclein found in two patients with amyotrophic lateral sclerosis induces aggregation into amyloid. Proc. Natl. Acad. Sci. USA *121*, e2309700120. https://doi.org/10.1073/pnas.2309700120.

31. Yang, S., Geiger, Y., Geerts, M., Eleveld, M.J., Kiani, A., and Otto, S. (2023). Enantioselective Self-Replicators. J. Am. Chem. Soc. *145*, 16889–16898. https://doi.org/10.1021/jacs.3c05472.

32. Chen, H., Abe, T., Chai, R., and Hiraoka, S. (2025). Selection of self-assembled configurational isomers from a dynamic library via a multivariant optimization process. Nat. Commun. *16*, 4387. https://doi.org/10.1038/s41467-025-59181-8.

33. Stingley, K.J., Carpenter, B.A., Kean, K.M., and Waters, M.L. (2023). Mismatched covalent and noncovalent templating leads to large coiled coil-templated macrocycles. Chem. Sci. *14*, 4935–4944. https://doi.org/10.1039/d3sc00231d.

34. Liu, Y., Wang, H., Shangguan, L., Liu, P., Shi, B., Hong, X., and Huang, F. (2021). Selective separation of phenanthrene from aromatic isomer mixtures by a water-soluble azobenzene-based macrocycle. J. Am. Chem. Soc. *143*, 3081–3085. https://doi.org/10.1021/jacs.1c01204.

35. Sholl, D.S., and Lively, R.P. (2016). Seven chemical separations to change the world. Nature *532*, 435–437. https://doi.org/10.1038/532435a.

36. Debnath, S., Das, M., Mondal, S., Sarkar, B.K., and Babu, G. (2025). Advances in chromatography: contemporary techniques and applications. Essent. Chem. *2*, 1–27. https://doi.org/10.1080/28378083.2025.2466624.

37. Li, J.R., Sculley, J., and Zhou, H.C. (2012). Metal-organic frameworks for separations. Chem. Rev. *112*, 869–932. https://doi.org/10.1021/cr200190s.

38. Wang, Z., Zhang, S., Chen, Y., Zhang, Z., and Ma, S. (2020). Covalent organic frameworks for separation applications. Chem. Soc. Rev. *49*, 708–735. https://doi.org/10.1039/c9cs00827f.

39. Osman, A.I., Chen, Z., Elgarahy, A.M., Farghali, M., Mohamed, I.M.A., Priya, A.K., Hawash, H.B., and Yap, P.S. (2024). Membrane Technology for Energy Saving: Principles, Techniques, Applications, Challenges, and Prospects. Adv. Energ. Sust. Res. *5*, 2400011. https://doi.org/10.1002/aesr.202400011.

40. Patel, K., Panchal, N., and Ingle, P. (2019). Review of Extraction Techniques Extraction Methods: Microwave, Ultrasonic, Pressurized Fluid, Soxhlet Extraction, Etc. Int. J. Adv. Res. Chem. Sci. *6*, 6–21. https://doi.org/10.20431/2349-0403.0603002.

41. Ramström, O., and Lehn, J.-M. (2002). Drug discovery by dynamic combinatorial libraries. Nat. Rev. Drug Discov. *1*, 26–36. https://doi.org/10.1038/nrd704.

42. Hinton, D.P., and Johnson, C.S., Jr. (1993). Diffusion ordered 2D NMR spectroscopy of phospholipid vesicles: determination of vesicle size distributions. J. Phys. Chem. *97*, 9064–9072. https://doi.org/10.1021/j100137a038.

43. Au-Yeung, H.Y., Cougnon, F.B.L., Otto, S., Pantoş, G.D., and Sanders, J.K.M. (2010). Exploiting donor–acceptor interactions in aqueous dynamic combinatorial libraries: exploratory studies of simple systems. Chem. Sci. *1*, 567–574. https://doi.org/10.1039/c0sc00307g.

44. Hunt, R.A.R., Ludlow, R.F., and Otto, S. (2009). Estimating Equilibrium Constants for Aggregation from the Product Distribution of a Dynamic Combinatorial Library. Org. Lett. *11*, 5110–5113. https://doi.org/10.1021/ol901656x.

45. Headen, T.F., Howard, C.A., Skipper, N.T., Wilkinson, M.A., Bowron, D.T., and Soper, A.K. (2010). Structure of $\pi - \pi$ Interactions in Aromatic Liquids. J. Am. Chem. Soc. *132*, 5735–5742. https://doi.org/10.1021/ja909084e.

46. Lee, C., Yan, H., Brus, L.E., Heinz, T.F., Hone, J., and Ryu, S. (2010). Anomalous lattice vibrations of single-and few-layer MoS2. ACS Nano *4*, 2695–2700. https://doi.org/10.1021/nn1003937.